meta-Selective Radical Acylation of Electron-rich Arenes

Yamato Goto,[1] Masaki Sano,[1] Yuto Sumida,[2]* and Hirohisa Ohmiya[3,4]*

[1] Division of Pharmaceutical Sciences, Graduate School of Medical Sciences, Kanazawa University, Kakuma-machi, Kanazawa 920-1192, Japan

[2] Laboratory of Chemical Bioscience, Institute of Biomaterials and Bioengineering, Tokyo Medical and Dental University (TMDU), 2-3-10 Kanda-Surugadai, Chiyoda-ku, Tokyo 101-0062, Japan

[3] Institute for Chemical Research, Kyoto University, Gokasho, Uji, Kyoto 611-0011, Japan

[4] JST, PRESTO, 4-1-8 Honcho, Kawaguchi, Saitama 332-0012, Japan

*e-mail: sumida.yuto@tmd.ac.jp; ohmiya@scl.kyoto-u.ac.jp

meta-Selective functionalisation of electron-rich arenes provides a non-traditional route to organic synthesis. In classical electrophilic aromatic substitution of electron-donating group-pendant arenes, functionalisation occurs according to *ortho*- and *para*-orientation. There have been numerous efforts to overcome this selectivity, and various synthetic methods have been developed, mainly based on transition metal catalysis. Here, we show a new N-heterocyclic carbene and organic photoredox cocatalysis for *meta*-selective acylation of electron-rich arenes. This approach proceeds without the directing groups or steric factors required in transition metal catalysis, resulting in precisely opposite regioselectivity from conventional approaches such as the Friedel–Crafts acylation. The catalytic system involves a sequence of single electron oxidation of an electron-rich arene followed by the radical–radical coupling between a ketyl radical and an arene radical cation. This protocol will lead to the expeditious synthesis of organic molecules that commonly require multiple steps and rare metals and promotes the construction of libraries of biologically active molecules.

The Friedel–Crafts reaction is one of the most popular chemical reactions, appearing in all organic chemistry textbooks. Since Friedel and Crafts reported the inorganic halide-catalysed

acylation of aromatic rings in 1877,[1,2] this protocol has been widely used from the laboratory to industrial level, for the synthesis of materials, natural products, and pharmaceutical agents. The Friedel–Crafts acylation reaction proceeds efficiently with electron-rich arenes via the generation of acylium cations promoted by an inorganic Lewis acid (Fig. 1a). The acyl group is introduced in the *ortho*- and *para*-positions to the electron-donating group of aromatic rings. Synthetic organic chemists have constructed complex aromatic rings according to this characteristic *ortho*- and *para*-selectivity of electrophilic aromatic substitution reactions. Therefore, selectivity overcoming this golden rule, i.e., *meta*-selective aromatic substitution reactions of electron-rich arenes, is a challenging process and provides a powerful toolbox for organic synthesis. In this context, transition metal-catalysed C–H activation strategies have emerged as a new methodology for achieving *meta*-selective functionalisation of aromatic rings.[3–6] The *meta*-selective C–H bond functionalisation has concomitantly evolved with the development of rationally designed directing groups and ligands for transition metal catalysts (Fig. 1b).[7–13] Despite the recent significant advances in this area, these strategies still require directing groups or steric factors on arenes.

There has been significant progress in N-heterocyclic carbene (NHC) catalysis involving the radical process via the single electron transfer (SET) event described by our group, Studer, and Scheidt, etc. in recent years.[14–32] The persistent radical, a ketyl radical, was catalytically generated from aldehydes or carboxylic acids under SET oxidative or reductive NHC catalysis, which enabled the radical–radical coupling with a transient alkyl radical based on the persistent radical effect (PRE)[33] to provide acylated products. We envisioned that this ketyl radical could couple with a radical cation[34,35] from the SET oxidation of an electron-rich arene (Fig. 1c). Controlling the reactivity of the arene radical cation and the selectivity of radical–radical coupling was expected to achieve *meta*-selective acylation of electron-rich arenes.

We established our working hypothesis of NHC/photoredox cocatalysed *meta*-selective acylation of the electron-rich arenes. Our reaction design initiates SET oxidation of electron-rich arene **I** to generate radical cation species **II** under photoredox catalysis (Fig. 1d). Meanwhile, the addition-elimination of acyl imidazole **III** with the NHC catalyst afforded acyl azolium intermediate **IV** and an imidazolide anion. The leaving group (**LG**), the imidazolide anion, not only serves as a carboxylic acid derivative to produce acyl azolium intermediate **IV**, but also works as a nucleophile to the arene radical cation **II** to furnish cyclohexadienyl radical **V**, which is temporarily buried in the *para*-position to achieve *meta*-

selective acylation. The key to the success of the desired process is that the **LG**-added cyclohexadienyl radical **V** undergoes the radical–radical coupling with the ketyl radical **VI**. The SET reduction of acyl azolium **IV** gave ketyl radical **VI** to close the photoredox cycle. The cyclohexadienyl radical **V** is a transient radical compared to the ketyl radical, whose different reactivity leads to the desired cross-selective radical–radical coupling. Consequently, re-aromatisation of the radical–radical coupling adduct **VII** provides *meta*-selective acylated product **VIII**, imidazole, and NHC to close the NHC catalytic cycle.
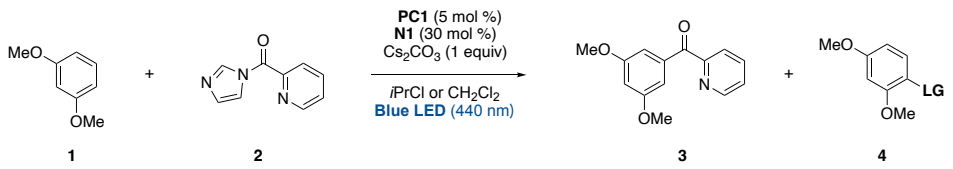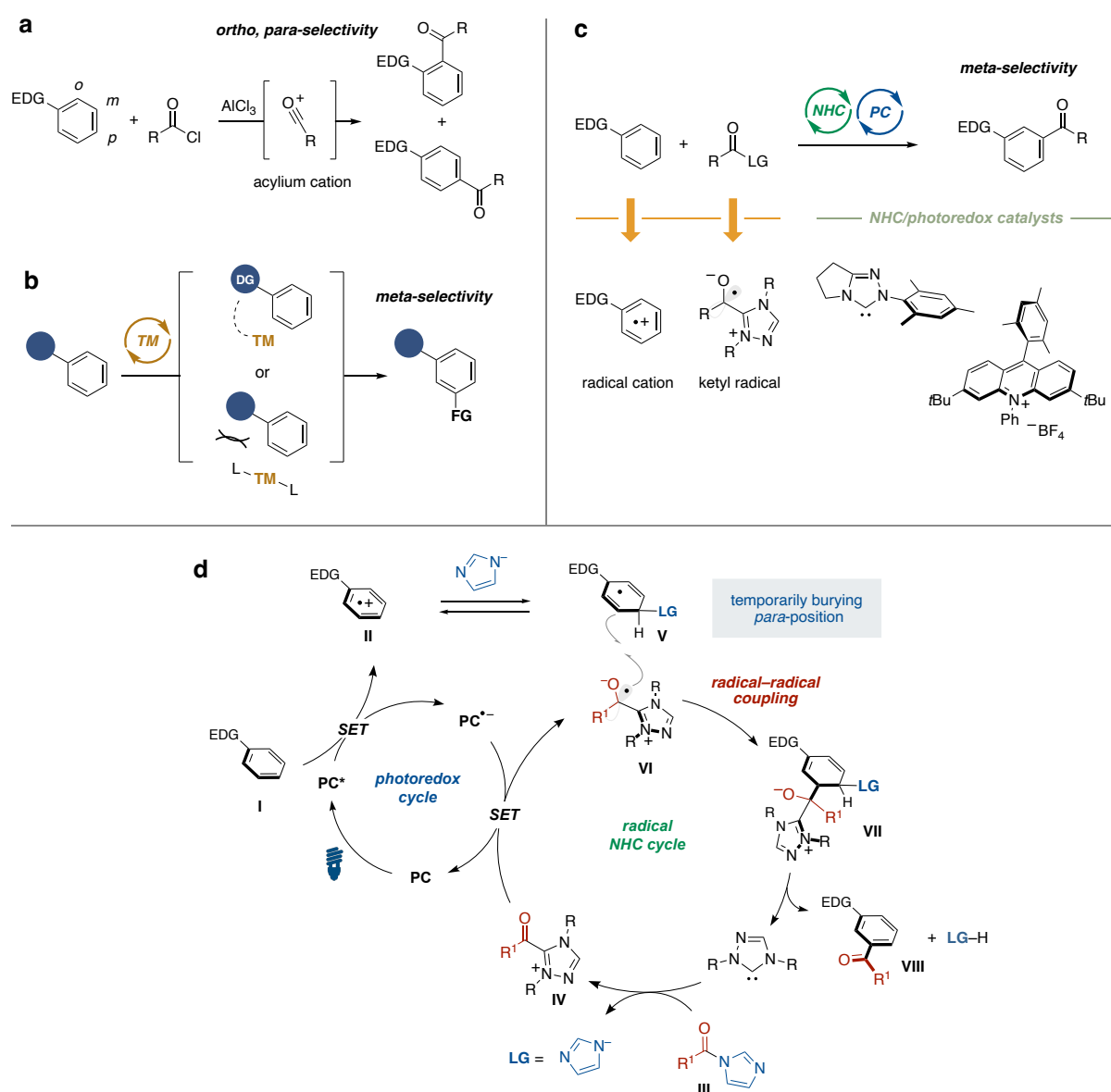

Fig. 1 | Regioselective functionalisation of arenes. a, *ortho*-, *para*-selective Friedel–Crafts acylation. EDG, electron donating group. **b**, Transition metal-catalysed *meta*-selective functionalisation. TM, transition metal. **c**, Cooperative NHC and photoredox-catalysed *meta*-selective acylation (this work). **d**, Reaction design.

3

We then embarked on evaluating the feasibility of our reaction design (Table 1). After extensive screening, we found adequate conditions that afforded *meta*-selective acylation product **3** in moderate yield using 1,3-dimethoxybenzene (**1**) as a model substrate, the acylation reagent **2**, the photocatalyst **PC1** (5 mol %), a Fukuzumi-type catalyst[36–38] showing high oxidation potential (E^*_{red} = +2.15 V vs SCE), triazole-based NHC catalyst **N1** (30 mol %), and cesium carbonate (1 equivalent) in 2-chloropropane under visible light irradiation (440 nm) (Table 1, entry 1). While the 1-(2,4-dimethoxyphenyl)-1*H*-imidazole **4a** generated via SET oxidation of the cyclohexadienyl radical **V** was obtained as a by-product in this reaction, no other regioselective isomers were observed. A slightly lower yield was observed in the case of dichloromethane as solvent (entry 2). In the screening of the photocatalyst, **PC2**, which has a relatively low oxidation potential (E^*_{red} = +1.65 V vs SCE) and high reduction potential ($E^{red}_{1/2}$ = –0.82 V vs SCE) in the radical anion state, yielded only a small amount of the target product (entry 3). In contrast, the *meta*-acylation proceeded with **PC3** and **PC4**, which have similar redox potentials to **PC1** (entries 4 and 5). These results suggest that the rapid single-electron oxidation process of the electron-rich arene is more important than the single-electron reduction process of the acyl azolium intermediate **IV** (Fig. 1d). When the NHC catalyst **N1** was replaced by structurally-small dimethyl triazole **N2**, the reaction was substantially less efficient (entry 6). A more nucleophilic thiazole-type carbene **N3** catalyst resulted in no reaction (entry 7).

Next, we explored the leaving group of the acylation reagent, which plays a dual role in the radical NHC catalysis. Benzimidazole **LG2** was used as the leaving group instead of imidazole **LG1**, giving the product in only trace amounts (entry 8). While the triazole **LG3** as a leaving group provided a decent yield, the 3-trifluoromethyltriazole **LG4**, which generated less nucleophilic anions *in situ*, resulted in no products (entries 9 and 10). Given the importance of **LG** as a nucleophile, we expected the addition of azoles or the pre-prepared azolide salt[39] would be beneficial for achieving a higher reaction efficiency due to increased initial concentration of the corresponding anions (Supplementary Fig. 2). Indeed, there was an obvious difference in the product yields when 1*H*-imidazole and 1*H*-1,2,4-triazole were used as additives, respectively (entries 11 and 12). The 1*H*-1,2,4-triazole as additive showed an improved result likely due to its lower nucleophilicity and higher leaving-group ability. A substoichiometric amount of easy-to-handle and prepare cesium 1,2,4-triazolide resulted in

comparable yield (entry 13). Consequently, the matching the rates of formation of acyl azolium intermediates and cyclohexadienyl radicals is important to achieve satisfactory result.

Table 1 | Screening of reaction conditions[a]

entry	deviation from standard conditions	yield (%)	
		3^b	$4^{b,c}$
1	*i*PrCl as solvent	48	42
2	CH_2Cl_2 as solvent	45	21
3	**PC2** instead of **PC1**	7^d	4
4	**PC3** instead of **PC1**	43^d	23
5	**PC4** instead of **PC1**	20^d	12
6	**N2** instead of **N1**	15^d	18
7	**N3** instead of **N1**	2^d	13
8	**LG2** instead of **LG1**	6^d	6
9	**LG3** instead of **LG1**	$31^{d,f}$	54
10	**LG4** instead of **LG1**	N.D.^{d,e}	51
11	1*H*-imidazole (1 equiv) as additive	$51^{g,h}$	19
12	1*H*-1,2,4-triazole (1 equiv) as additive	$65^{g,h}$	30
13	cesium 1,2,4-triazolide (70 mol %) instead of Cs_2CO_3	$66^{g,f}$	34

PC1 **PC2** **PC3** **PC4**

N1 **N2** **N3**

LG1 **LG2** **LG3** **LG4** cesium 1,2,4-triazolide
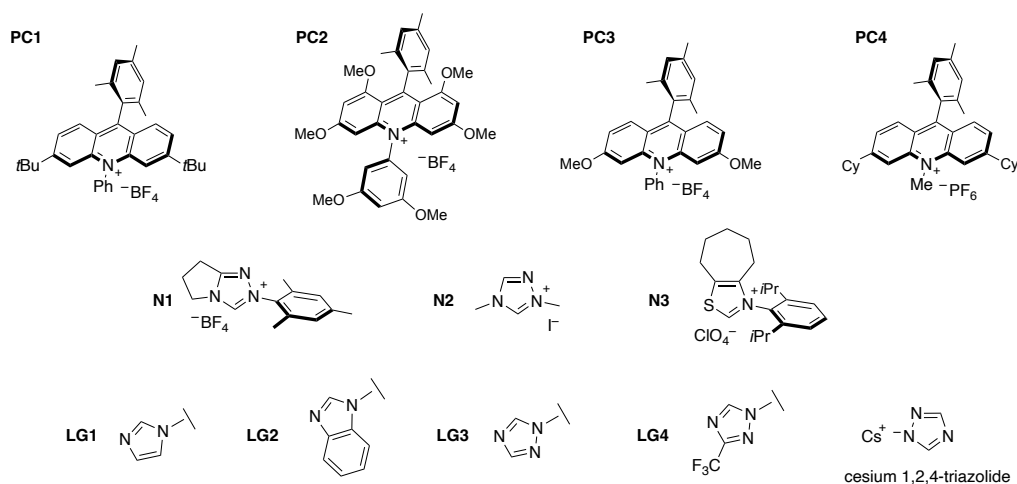
[a] Reaction was carried out with 1,3-dimethoxybenzene (**1**) (0.05 mmol), acyl imidazole **2** (0.15 mmol), **PC1** (5 mol %), **N1** (30 mol %), and Cs_2CO_3 (0.05 mmol) in 2-chloropropane or dichloromethane (0.15 mL) under 440 nm (Kessil lamp equipped with PhotoRedOx Duo) irradiation for 16 h. [b] ^{1}H NMR yield. [c] Total amount of azole adducts. [d] 2-Chloropropane was used as solvent. [e] Not detected. [f] Direct irradiation. [g] Dichloromethane was used as solvent. [h] Reaction was carried out in 0.2 mmol scale of 1,3-dimethoxybenzene (**1**) for 20 h.

With the discovered *meta*-acylation conditions based on NHC/photoredox catalysis, we moved to the exploration of the reaction scope (Fig. 2). The products were basically obtained as single regioisomer unless otherwise noted. Mono-alkoxy substituted electron-rich arenes, of which the Friedel–Crafts acylation commonly progresses with *ortho*- and *para*-orientation, gave the corresponding products **5**–**8** using our protocols. Easily deprotectable substrates such as MOM and TBS groups also yielded *meta*-acylation products **9** and **10** without loss of their units, although not in excellent yields. Similarly, the reaction of 1,3-disubstituted electron-rich arenes, which also usually occurs at the *ortho*-position of the electron-donating substituent, proceeded efficiently to produce *meta*-acylated arenes **3** and **11**–**15**. Notably, despite the O-allyl group being readily deprotected under transition metal catalytic conditions, and its conversion to phenol, the product **14** is obtained under this radical NHC catalysis. This *meta*-selective acylation has been prone to depend on the electron abundance of the arenes, with halogenated arenes and pyridine-based arenes showing poor reactivity, while trisubstituted arenes with more electron-rich substituents proceeding efficiently (**16**–**22**). The regioselectivity differed depending on the size of the substituent in 1,2-disubstituted arene. 1-Chloro-2-methoxybenzene showed no regioselectivity giving a mixture of C3 and C5-

acylated products **17**, while *meta*-acylation proceeded almost selectively with the *t*Bu group **18**. Acenes revealed excellent reactivity, yielding the corresponding acylation products with high generality and selectivity. This outcome supports our hypothesis that the reaction pathway involves cyclohexadienyl radical **V** generated via the dearomatisation of the electron-rich arenes.

The regioselective acylation progressed at the 4-position of 2-methoxynaphthalene to furnish the product **23** in 95% yield (Fig. 2, middle). The halogen and acetyl group-substituted methoxynaphthalenes provided regioselective acylated products **24** and **25**. Acylation also proceeded with non-substituted naphthalene or 2-ethyl naphthalene, giving a mixture of 4- and 2-acylated products **26** and **26′** in the case of naphthalene, or 4-acylated product **27** as a major product with unidentifiable by-products. Polyacenes, such as phenanthrene and anthracene, were applicable to form mono-acylated products **28** and **29**. Similar to the pyridine derivative, the π-extended heteroarenes, 6-methoxyquinoline and 5-methoxyindole, could participate in this catalytic system giving **30** and **31**. 2-Methoxynaphthalene often serves as an important motif in bioactive compounds. Therefore, to probe our acylation protocol practical, we examined the late-stage functionalisation of several pharmaceuticals. Delightfully, the marketed medicinal reagents, including agomelatine, nabumetone, and naproxen, delivered the single regioisomeric adducts **32–34**, respectively. Moreover, SN-38, antineoplastic drug having electron-rich quinoline skeleton, was also convertible to acylated product **35** with high regioselectivity.

We next investigated the range of the applicable carboxylic acid derivatives (Fig. 2, bottom). The products were obtained as single *meta*-isomer. The reaction of 2,6-dimethoxytoluene with aroyl imidazoles derived from pyridine carboxylic acids and 2-quinoline carboxylic acid provided the corresponding diaryl ketones **36–39** in high yields. When the reaction of electron-rich arenes with aromatic carboxylic acid-derived aryl imidazoles was examined, *meta*-acylated products were obtained in moderate yields regardless of the electronic feature of the aromatic rings (**40–45**). Using 2-methoxynaphthalene as a substrate, the substituent effect of acyl imidazole was more prominent than that of the simple arene. While the acyl imidazoles having electron-withdrawing groups including chloride, nitrile, and trifluoromethyl on aromatic rings afforded 4-acylation products **46–48** with high efficiency, electronically-neutral and donating groups were ineffective, and moderate yields of products were obtained (**49–52**). In addition to being superb substrates, 2-quinoline and 2-pyridine carboxylic acids afforded excellent

yields, and other heteroarenes, 2-furyl and 2-thiophenyl carboxylic acids, were available as acylation reagents (**53**–**56**). The electron-deficient acyl imidazoles basically gave good outcome, which is attributable to the lifetime and reactivity of the ketyl radical based on captodative effect. 2-Naphthoic acid, 2-bromobenzoic acid, and 3,5-disubstituted benzoic acids afforded the acylated products **57**–**60** in moderate to excellent yields. When reacted with 2-methoxynaphthalene, *primary* aliphatic carboxylic acids also became the choice of acylating reagents. Although the installation of the alkanoyl group was performed with low efficiency because of the low reactivity of the corresponding ketyl radical, acetylation using acetic acid proceeded to give the acetylated product **63** as well as acylated products **61** and **62**. Lithocholic acid, a type of bile acid, can apply as alkanoylation reagent to deliver **64** in similar fashion.
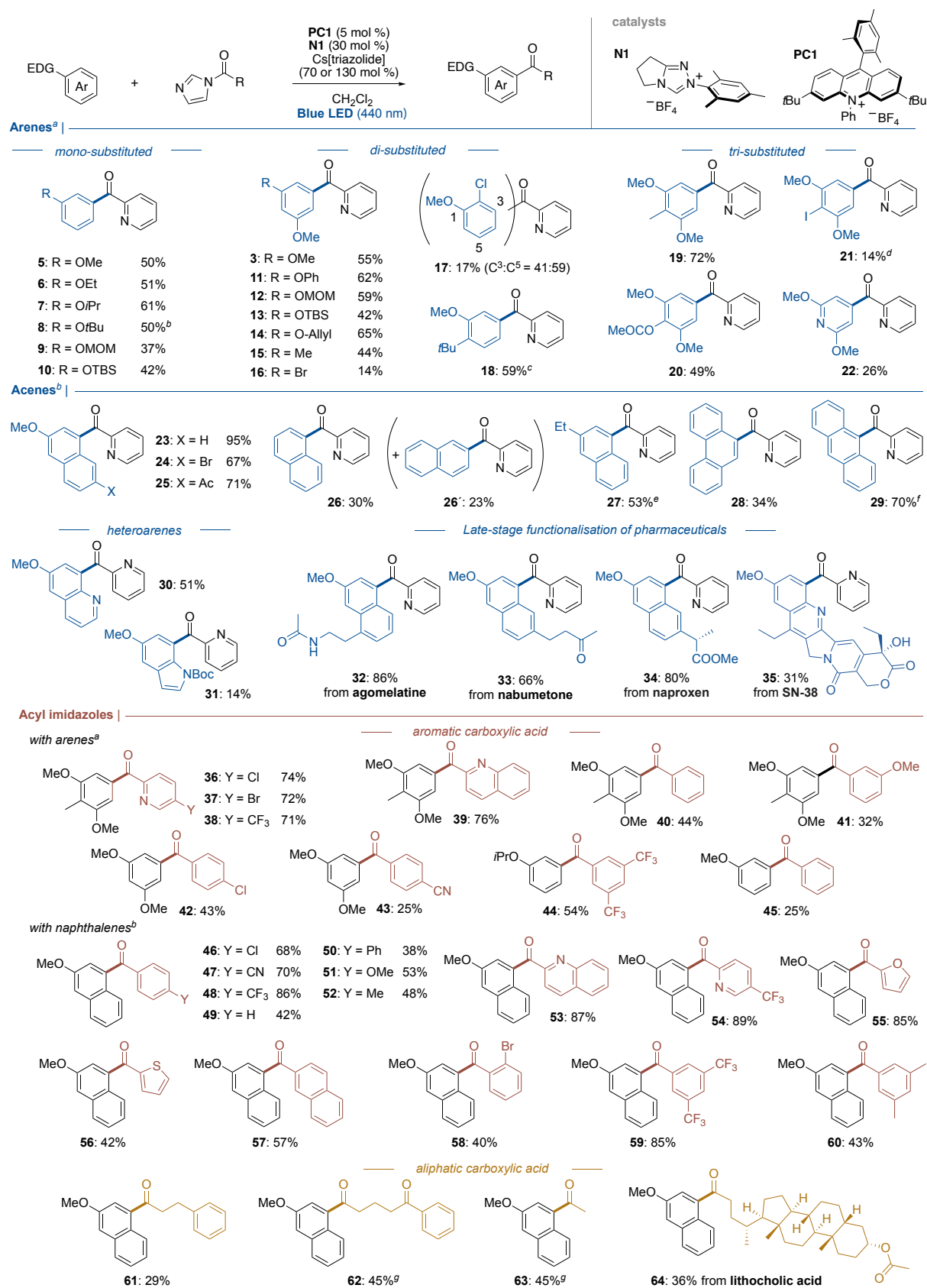
Fig. 2 | Regioselective acylation of various substrates. [a] Reaction was carried out with arene (0.2 mmol), acyl imidazole (0.6 mmol), **PC1** (5 mol %), **N1** (30 mol %), and cesium 1,2,4-triazolide (130 mol %) in dichloromethane (0.6 mL) under 440 nm

(Kessil lamp equipped with PhotoRedOx Duo) irradiation for 20 h. [b] **N1** (20 mol %), cesium 1,2,4-triazolide (70 mol %), and acyl imidazole (0.3 mmol) were used. [c] A small amount of para-acylation production was obtained. [d] Trace amount of inseparable deiodinated product was a contaminant. [e] 53% (C4 : other isomers = 58:42) of the product was observed. [f] A small amount of unidentified compounds was observed. [g] 390 nm LED light was used as a light source.

Additional computational approaches and an experiment were performed to support our working hypothesis. The natural population analysis of the anisole-delivered radical cation revealed that the initial nucleophilic addition of imidazole mainly occurs at the *para*-position (Fig. 3a). The small amount of 4-azolide anisole adduct was observed as by-product on the NHC/photoredox catalyzed acylation of anisole, which supported the computational analysis. Practically, the nucleophile potentially also attacks the *ortho*-position to provide the regioisomeric mixture of cyclohexadienyl radicals **65a** and **65b**.[35,37] The evaluation of nucleophilic addition step of azolide anion to arene radical cation based on the computational study revealed that the reaction at C4 (*para*)- or C2 (*ortho*)-position to generate the cyclohexadienyl radical **65a** or **65b** were favourable compared to the reaction of the most cationic C1-position because of the steric hindrance or C3-position as indicated by the charge density of arene radical cation (Fig. 3b). Considering the spin density distribution of the cyclohexadienyl radical **65a** or **65b**, the radical–radical coupling with the ketyl radical proceeded at the *meta*-position in each case. Although the highest spin density in intermediate **65a** is C1, the radical–radical coupling would not occur due to steric hindrance. Correspondingly, the calculated charge density of the radical cation generated from 2-methoxynaphthalene demonstrated that the positively charged and less hindered C1 position is kinetically preferred for the nucleophilic addition of azolide anions.[40] The C4 position of the resultant radical **66** after nucleophilic addition showed a higher spin density and was thus favorable for the radical–radical coupling (Fig. 3c).

We also evaluated the feasibility of our proposed reaction pathway with a computational method to gain mechanistic details and energy profiles (Fig. 3d). Each step from the radical cation of anisole to the product was calculated for the pathway associated with the imidazolide and triazolide anions, respectively. For the azolide anion addition step, the activation barrier for **TS1** was 5.8 kcal/mol compared to 20.9 kcal/mol for imidazole, which is more favourable for triazole based on the difference in ion pair stability. The radical–

radical coupling progress between the generated cyclohexadienyl radical **INT1** and ketyl radical via **TS2** (17.4 kcal/mol for triazole, 19.6 kcal/mol for imidazole, respectively) to afford **INT2**. Although the triazole-associated pathway is slightly more favourable, both give reasonable values. The subsequent NHC elimination from **INT2** had a low barrier, and the resulting **INT3** was largely stabilized. The deprotonation step with imidazolide anion, which is relatively abundant and the strong base in this reaction, gave enolate intermediate **INT4**. The final rearomatisation step, enolate intermediate **INT4**, proceeded readily in both paths, giving a *meta*-acylated product.

Additional experimental mechanistic studies including TEMPO experiment and Stern–Volmer plot were carried out to obtain insights on the SET event (supplementary Figs. 4 and 5). These results suggest that this catalytic system involves radical processes and SET oxidation of electron-rich arenes by excited **PC1** catalyst.[35,37] Moreover, no desired product was obtained when aryl imidazole **4a**, a by-product formed via oxidation of the cyclohexadienyl radical, was subjected to the optimised conditions (Fig. 3e). This indicates that **4a** is an off-cycle product of radical NHC catalysis, not an intermediate in the *meta*-acylation pathway.
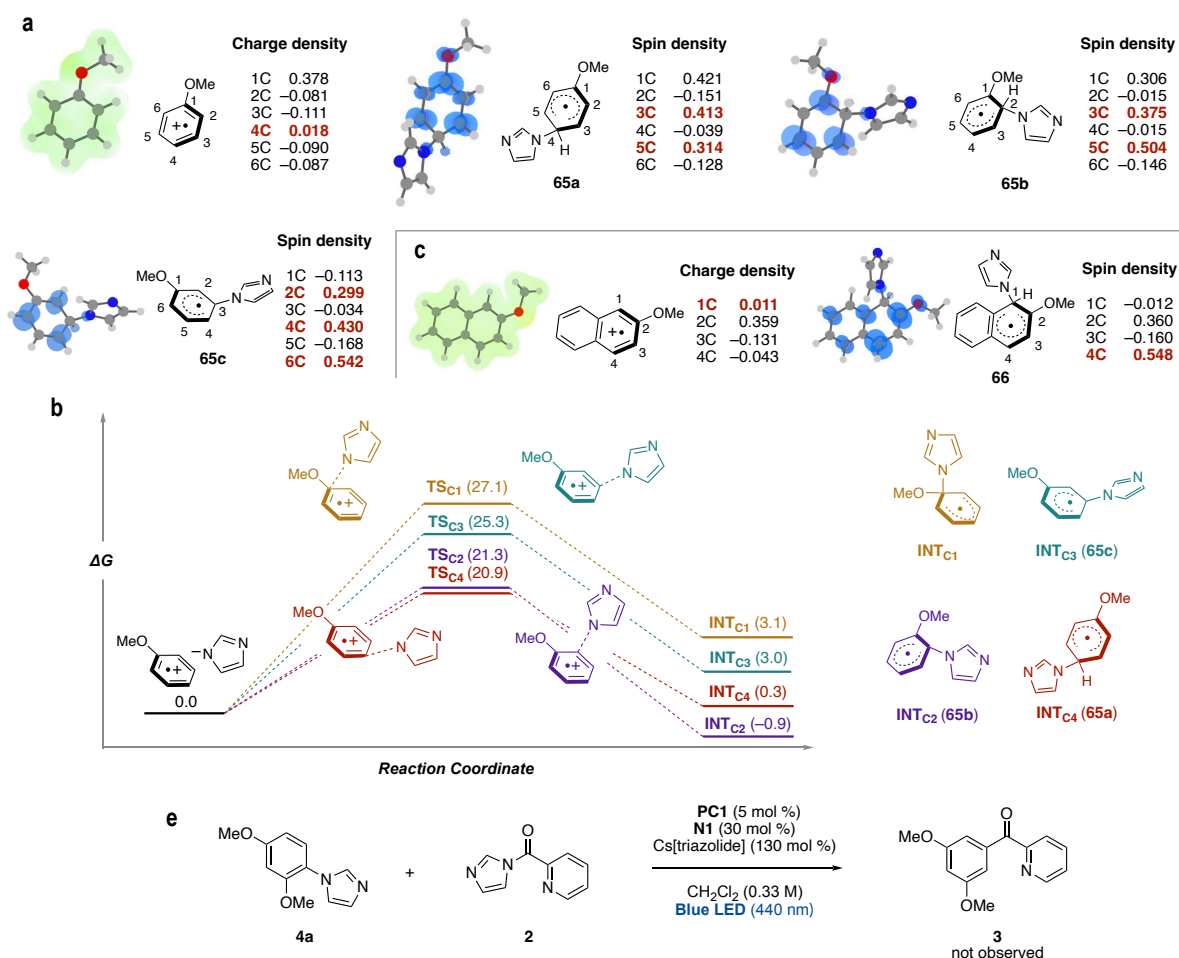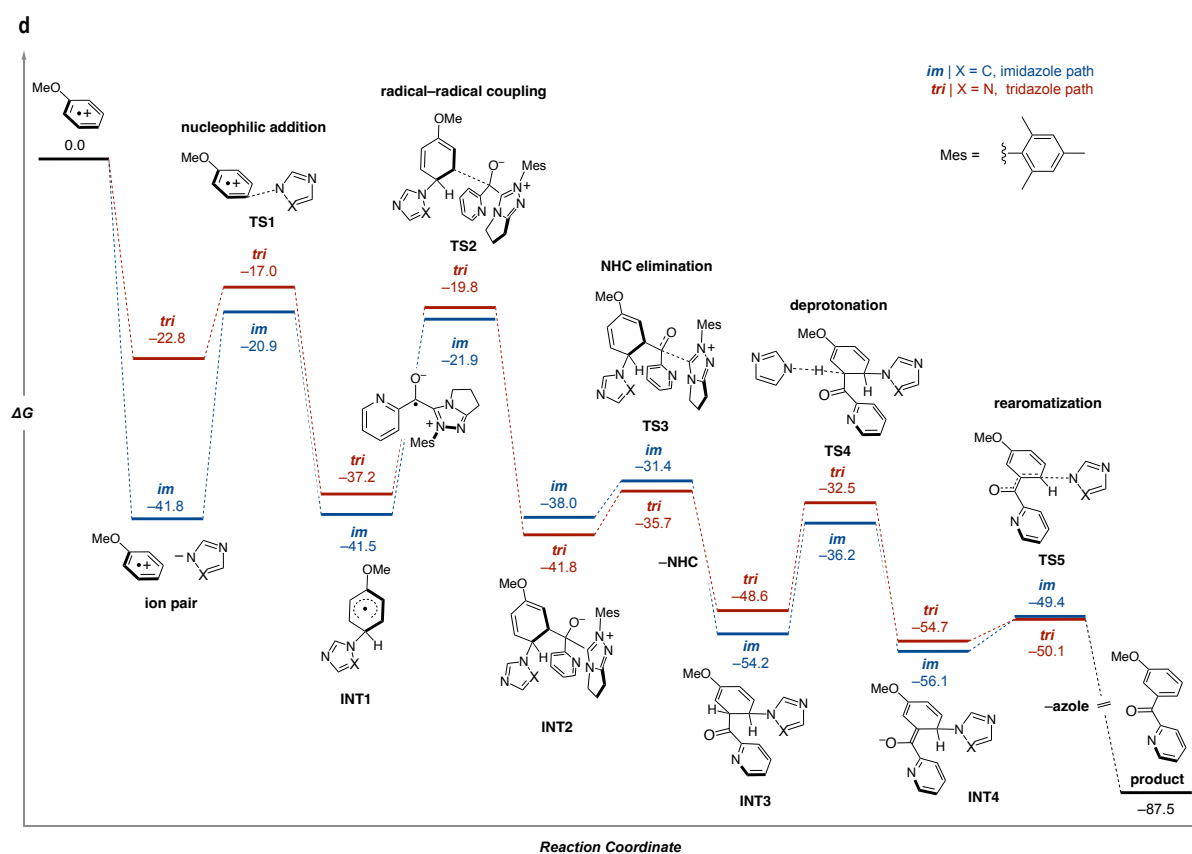
Fig. 3 | Mechanistic study. a, The charge densities of radical cations and the spin densities of cyclohexadienyl radicals **65a**, **65b**, and **65c** were calculated at the ωB97X-D/def2-TZVPP, SMD (dcm) level of theory. **b,** Regioselectivity for nucleophilic addition step of imidazolide anion as a nucleophile to radical cation of anisole. DFT calculations were carried out at the (U)M06-2X/6-311+G(d,p)/SMD (dcm)//(U)M06-2X/6-31+G(d,p)_SMD(dcm) level of theory. **c,** The charge density of radical cation and the spin density of cyclohexadienyl radical **66** were calculated at the ωB97X-D/def2-TZVPP, SMD (dcm) level of theory.   **d,** Energy profiles for the proposed pathway. The unit of Gibbs free energies is kcal/mol. DFT calculations were carried out at the (U)M06-2X/6-311+G(d,p)_SMD(dcm)//(U)M06-2X/6-31+G(d,p)_SMD(dcm) level of theory. The reaction pathway using imidazolide anion (blue line) and triazolide anion (red line). **e,** Reaction was carried out with **4a** (0.1 mmol), **2** (0.3 mmol), **PC1** (5 mol %), **N1** (30 mol %), and cesium 1,2,4-triazolide (130 mol %) in dichloromethane (0.3 mL) under 440 nm (Kessil lamp equipped with PhotoRedOx Duo) irradiation for 20 h.

We have developed the NHC and organic photoredox cooperative catalytic *meta*-selective acylation of electron-rich arenes. The catalytic system involves a nucleophilic addition of an azolide anion to the radical cation species produced by single electron oxidation of the electron-rich arenes. The nucleophile, the azolide anion, is delivered from the acylation reagent, acyl imidazole, via addition/elimination with an NHC catalyst. The desired *meta*-acylation was achieved based on the cross-selective radical–radical coupling of the cyclohexadienyl radical formed by the nucleophilic addition with the persistent radical, the ketyl radical, via single electron reduction of the acyl azolium intermediate. This protocol overturns the *ortho*- and *para*-orientation of electron-rich arenes, as in the Friedel–Crafts acylation. We expect to expand this process to further reaction processes, enabling the development of transformative methodology and the construction of new chemical spaces facilitating drug discovery.

Data availability

Details on the procedures, optimization and characterization including spectra of new compounds and compounds made using the reported method, are available in the Supplementary Information.

References

1. Friedel, C., Crafts, J.-M. *Compt. Rend.* **84**, 1450–1454 (1877).

2. Crafts, J. M., Ador, E. *Ber.* **10**, 2173 (1877).

3. Leitch, J. A. & Frost, C. G. Ruthenium-catalysed σ-activation for remote *meta*-selective C–H functionalisation. *Chem. Soc. Rev.* **46**, 7145–7153 (2017). DOI: 10.1039/c7cs00496f

4. Gandeepan, P. & Ackermann, L. Transient Directing Groups for Transformative C–H Activation by Synergistic Metal Catalysis. *Chem* **4**, 199–222 (2018). DOI: 10.1016/j.chempr.2017.11.002

5. Mihai, M. T., Genov, G. R. & Phipps, R. J. Access to the meta position of arenes through transition metal catalysed C–H bond functionalisation: a focus on metals other than palladium. *Chem. Soc. Rev.* **47**, 149–171 (2018). DOI: 10.1039/C7CS00637C

6. Dey, A., Sinha, S. K., Achar, T. K. & Maiti, D. Accessing Remote *meta*- and *para*-C(sp^2)−H Bonds with Covalently Attached Directing Groups. *Angew. Chem. Int. Ed.* **58**, 10820–10843 (2019). DOI: 10.1002/anie.201812116

7. Phipps, R. J. & Gaunt, M. J. A Meta-Selective Copper-Catalysed C–H Bond Arylation. *Science* **323**, 1593–1597 (2009). DOI: 10.1126/science.1169975

8. Leow, D., Li, G., Mei, T.-S. & Yu, J.-Q. Activation of remote *meta*-C–H bonds assisted by an end-on template. *Nature* **486**, 518–522 (2012). DOI: 10.1038/nature11158

9. Wang, X.-C. *et al.* Ligand-enabled meta-C–H activation using a transient mediator. *Nature* **519**, 334–338 (2015). DOI: 10.1038/nature14214

10. Kuninobu, Y., Ida, H., Nishi, M. & Kanai, M. A meta-selective C–H borylation directed by a secondary interaction between ligand and substrate. *Nat. Chem.* **7**, 712–717 (2015). DOI: 10.1038/nchem.2322

11. Shi, H., Herron, A. N., Shao, Y., Shao, Q. & Yu, J.-Q. Enantioselective remote *meta*-C–H arylation and alkylation via a chiral transient mediator. *Nature* **558**, 581–585 (2018). DOI: 10.1038/s41586-018-0220-1

12. Ramadoss, B., Jin, Y., Asako, S. & Ilies, L. Remote steric control for undirected *meta*-selective C–H activation of arenes. *Science* **375**, 658–663 (2022). DOI: 10.1126/science.abm7599

13. Cao, H., Cheng, Q. & Studer, A. Radical and ionic *meta*-C–H functionalization of pyridines, quinolines, and isoquinolines. *Science* **378**, 779–785 (2022). DOI: 10.1126/science.ade6029

14. Ishii, T., Nagao, K. & Ohmiya, H. Recent advances in N-heterocyclic carbene-based radical catalysis. *Chem. Sci.* **11**, 5630–5636 (2020). DOI: 10.1039/D0SC01538E

15. Ohmiya, H. N-Heterocyclic Carbene-Based Catalysis Enabling Cross-Coupling Reactions. *ACS Catal.* **10**, 6862–6869 (2020). DOI: 10.1021/acscatal.0c01795

16. Liu, K., Schwenzer, M. & Studer, A. Radical NHC Catalysis. *ACS Catal.* 11984–11999 (2022). DOI: 10.1021/acscatal.2c03996

17. Bay, A. V. & Scheidt, K. A. Single-electron carbene catalysis in redox processes. *Trends Chem.* **4**, 277–290 (2022). DOI: 10.1016/j.trechm.2022.01.003

18. Ishii, T., Kakeno, Y., Nagao, K. & Ohmiya, H. N-Heterocyclic Carbene-Catalysed Decarboxylative Alkylation of Aldehydes. *J. Am. Chem. Soc.* **141**, 3854–3858 (2019). DOI: 10.1021/jacs.9b00880

19. Ishii, T., Ota, K., Nagao, K. & Ohmiya, H. N-Heterocyclic Carbene-Catalysed Radical Relay Enabling Vicinal Alkylacylation of Alkenes. *J. Am. Chem. Soc.* **141**, 14073–14077 (2019). DOI: 10.1021/jacs.9b07194

20. Davies, A. V., Fitzpatrick, K. P., Betori, R. C. & Scheidt, K. A. Combined Photoredox and Carbene Catalysis for the Synthesis of Ketones from Carboxylic Acids. *Angew. Chem. Int. Ed.* **59**, 9143–9148 (2020). DOI: 10.1002/anie.202001824

21. Kakeno, Y., Kusakabe, M., Nagao, K. & Ohmiya, H. Direct Synthesis of Dialkyl Ketones from Aliphatic Aldehydes through Radical N-Heterocyclic Carbene Catalysis. *ACS Catalysis* **10**, 8524-8529 (2020). DOI: 10.1021/acscatal.0c02849

22. Zuo, Z., Daniliuc, C. G. & Studer, A. Cooperative NHC/Photoredox Catalysed Ring-Opening of Aryl Cyclopropanes to 1-Aroyloxylated-3-Acylated Alkanes. *Angew. Chem. Int. Ed.* **60**, 25252–25257 (2021). DOI: 10.1002/anie.202110304

23. Matsuki, Y. *et al.* Aryl radical-mediated N-heterocyclic carbene catalysis. *Nat. Commun.* **12** (2021). DOI: 10.1038/s41467-021-24144-2

24. Liu, K. & Studer, A. Direct α-Acylation of Alkenes via N-Heterocyclic Carbene, Sulfinate, and Photoredox Cooperative Triple Catalysis. *J. Am. Chem. Soc.* **143**, 4903–4909 (2021). DOI: 10.1021/jacs.1c01022

25. Meng, Q.-Y., Lezius, L. & Studer, A. Benzylic C−H acylation by cooperative NHC and photoredox catalysis. *Nat. Commun.* **12** (2021). DOI: 10.1038/s41467-021-22292-z

26. Sato, Y. *et al.* Light-Driven N-Heterocyclic Carbene Catalysis Using Alkylborates. *ACS Catal.* 12886–12892 (2021). DOI: 10.1021/acscatal.1c04153

27. Ren, S.-C. *et al.* Carbene and photocatalyst-catalysed decarboxylative radical coupling of carboxylic acids and acyl imidazoles to form ketones. *Nature Commun.* **13** (2022). DOI: 10.1038/s41467-022-30583-2

28. Bay, A. V., Farnam, E. J. & Scheidt, K. A. Synthesis of Cyclohexanones by a Tandem Photocatalyzed Annulation. *J. Am. Chem. Soc.* **144**, 7030–7037 (2022). DOI: 10.1021/jacs.1c13105

29. Yu, X., Meng, Q. Y., Daniliuc, C. G. & Studer, A. Aroyl Fluorides as Bifunctional Reagents for Dearomatizing Fluoroaroylation of Benzofurans. *J. Am. Chem. Soc.* (2022). DOI: 10.1021/jacs.2c01735

30. Han, Y.-F. *et al.* Photoredox cooperative N-heterocyclic carbene/palladium-catalysed alkylacylation of alkenes. *Nat. Commun.* **13**, 5754 (2022). DOI:10.1038/s41467-022-33444-0

31. Yang, W., Hu, W., Dong, X., Li, X. & Sun, J. N-Heterocyclic Carbene Catalyzed γ-Dihalomethylenation of Enals by Single-Electron Transfer. *Angew. Chem. Int. Ed.* **55**, 15783-15786 (2016). DOI: 10.1002/anie.201608371

32. DiRocco, D. A. & Rovis, T. Catalytic Asymmetric α-Acylation of Tertiary Amines Mediated by a Dual Catalysis Mode: N-Heterocyclic Carbene and Photoredox Catalysis. *J. Am. Chem. Soc.* **134**, 8094-8097 (2012). DOI:10.1021/ja3030164

33. Leifert, D. & Studer, A. The Persistent Radical Effect in Organic Synthesis. *Angew. Chem. Int. Ed.* **59**, 74–108 (2020). DOI: 10.1002/anie.201903726

34. Ohkubo, K., Mizushima, K., Iwata, R. & Fukuzumi, S. Selective photocatalytic aerobic bromination with hydrogen bromide via an electron-transfer state of 9-mesityl-10-methylacridinium ion. *Chem. Sci.* **2**, 715 (2011). DOI:10.1039/c0sc00535e

35. Romero, N. A., Margrey, K. A., Tay, N. E. & Nicewicz, D. A. Site-selective arene C-H amination via photoredox catalysis. *Science* **349**, 1326–1330 (2015). DOI: 10.1126/science.aac9895

36. Fukuzumi, S. *et al.* Electron-Transfer State of 9-Mesityl-10-methylacridinium Ion with a Much Longer Lifetime and Higher Energy Than That of the Natural Photosynthetic Reaction Center. *J. Am. Chem. Soc.* **126**, 1600–1601 (2004). DOI:10.1021/ja038656q

37. Margrey, K. A., McManus, J. B., Bonazzi, S., Zecri, F. & Nicewicz, D. A. Predictive Model for Site-Selective Aryl and Heteroaryl C–H Functionalisation via Organic Photoredox Catalysis. *J. Am. Chem. Soc.* **139**, 11288–11299 (2017). DOI:10.1021/jacs.7b06715

38. Yan, H., Song, J., Zhu, S. & Xu, H.-C. Synthesis of Acridinium Photocatalysts via Site-Selective C–H Alkylation. *CCS Chem.* **3**, 317–325 (2021). DOI: 10.31635/ccschem.021.202000743

39. Truong, C. C., Kim, J., Lee, Y. & Kim, Y. J. Well-Defined Cesium Benzotriazolide as an Active Catalyst for Generating Disubstituted Ureas from Carbon Dioxide and Amines. *ChemCatChem* **9**, 247–252 (2017). DOI:10.1002/cctc.201601320

40. Ji, P. *et al.* Selective skeletal editing of polycyclic arenes using organophotoredox dearomative functionalisation. *Nat. Commun.* **13** (2022). DOI:10.1038/s41467-022-32201-7

Acknowledgements

Author contributions

Y.G., M.S., Y.S., and H.O. designed, performed and analysed the experiments. Y.S. and H.O. co-wrote the manuscript. All authors contributed to discussions.

Competing financial interests

The authors declare no competing financial interests.

Additional information

Supplementary information The online version contains supplementary material available at http://doi.org/10.1038/.

Correspondence and requests for materials should be addressed to H.O or Y.S.